Robust Vehicle Localization Using Entropy-Weighted Particle Filter-based Data Fusion of Vertical and Road Intensity Information for a Large Scale Urban Area

Hyungjin Kim, Bingbing Liu, Chi Yuan Goh, Serin Lee, *Senior Member, IEEE*, and Hyun Myung, *Senior Member, IEEE*

***Abstract*—This letter proposes a robust vehicle localization method based on a prior point cloud in urban area. The high resolution point cloud collected six months ago is provided from Singapore Land Authority around One-north area in Singapore, because the data are outdated there are many changed aspects of the environment such as redrawn road markings, construction areas, and changing tree shapes. In response, this paper proposes a novel fusion algorithm based on a particle filter using vertical and road intensity information for robust localization. Whereas the state-of-the-art fusion algorithm focus on optimization of the vehicle pose based on multiple measurements, the proposed method estimates a robust vehicle pose by considering the reliability of each feature from the prior map. We also propose an efficient management strategy of a grid map that includes multilayer vertical and road intensity information for real-time operation. A sensor system equipped on a vehicle consists of 32 channels of 3D Light Detection And Ranging, IMU, wheel odometry, which are used for the proposed algorithm. RTK-GPS, wheel odometry, and iterative closest point algorithm are utilized by using a graph-structure optimization method in off-line for estimating ground truth. The total data set for the demonstration is collected in a 19.9 km way in an urban area. The proposed approach has successfully performed an autonomous vehicle driving in an urban area.**

***Index Terms*—Autonomous vehicle navigation, field robots, localization, sensor fusion.**

Manuscript received September 11, 2016; revised December 11, 2016; accepted February 3, 2017. Date of publication February 23, 2017; date of current version March 17, 2017. This letter was recommended for publication by Associate Editor A. Elfes and Editor J. Roberts upon evaluation of the reviewers' comments. This work was supported in part by the Industrial Convergence Core Technology Development Program (10063172, Development of Robot Intelligence Technology for mobility with learning capability toward robust and seamless indoor and outdoor autonomous navigation) funded by the Ministry of Trade, Industry & Energy (MOTIE), South Korea, and in part by the Technology Innovation Program (10045252, Development of Robot Task Intelligence Technology) funded by the MOTIE, South Korea.

H. Kim and H. Myung are with the Urban Robotics Laboratory, Korea Advanced Institute of Science and Technology, Daejeon 34141, South Korea (e-mail: hjkim86@kaist.ac.kr; hmyung@kaist.ac.kr).

B. Liu, C. Y. Goh, and S. Lee are with the Department of Autonomous Vehicle, Institute for Infocomm Research, A*star, Singapore 138632 (e-mail: bliu@i2r.a-star.edu.sg; gohcy@i2r.a-star.edu.sg; serin-lee@i2r.a-star.edu.sg).

This letter has supplementary downloadable material available at http://ieeexplore.ieee.org, provided by the authors. The Supplemental Material contains a video clip for the proposed localization method using entropy-weighted particle filter. This material is 9.56 MB in size.

Color versions of one or more of the figures in this letter are available online at http://ieeexplore.ieee.org.

Digital Object Identifier 10.1109/LRA.2017.2673868

I. Introduction

THE problem of autonomous vehicle localization based on a prior point cloud has been intensively researched in the past decade. There are two general approaches for prior point cloud based localization using 3D LiDAR (Light Detection And Ranging) sensors. One approach utilizes road intensity information such as road markings [1]. The other uses vertical information of the point cloud such as buildings and trees [2], [3]. For high accuracy localization, a precise 3D point cloud is needed for both approaches. Recently, many map measurement companies provide precise point cloud map databases for autonomous vehicles collected by their own equipment and system, e.g., Mobile Mapping System (MMS) by Mitsubishi Electric Corporation [4] and Aisan Technology Company [5]. Since the equipment for a precise map is expensive and the data volume is enormous, it is challenging to collect a precise and up-to-date point cloud map frequently. Thus, a high-precision 3D point cloud for prior map-based localization is easily outdated. Thus, both general approaches have a limitation in terms of providing a fundamental solution for localization. For these reasons, robustness is one of the important issues for point cloud map-based localization.

Since being successfully implemented in the 2007 DARPA Urban Challenge for localization [6], [7], road intensity data are generally utilized for vehicle localization in urban areas [8]. As road intensity feature data in urban areas mainly consist of road markings such as lines, arrows, and crosses, the data can provide highly precise and constant information. Therefore, road intensity feature-based localization is possible to centimeter accuracy [1]. Moreover, it has been verified at day/night time and even in rain [1], [9]. However, the road intensity features can be regionally changed due to road work or redrawn road markings. This induces significant localization error.

On the other hand, there are many vertical feature-based localizations in indoor areas as well as urban areas [1], [10]. Although vertical features in urban areas include various noise data from pedestrians, cars, and seasonal change of trees, they are useful in areas where road intensity data are insufficient such as parks, off-road areas, and indoors. In addition, the vertical features do not frequently change overall, unlike road intensity features because they are extracted from buildings and trees.

Since the most important factor in autonomous vehicles is robustness for safety, the vehicles utilize not only a multi-sensor

system but also various features from multiple sensors [8]. Yoneda *et al.* [11], [12] proposed urban road localization using multiple layer maps and line segment matching. The vehicle pose is estimated using multi-layer ICP (Iterative Closest Point) matching followed by line marker matching from a precise point cloud database. Deusch *et al.* [13] and Caron *et al.* [14] proposed multi-sensor localization based on a particle filter. These studies focus on optimization of the vehicle pose based on multiple measurements and sensors. However, they do not consider reliability of the prior map.

In response, this letter proposes an efficient fusion algorithm using both road intensity and vertical features by considering the reliability of each feature map. In this letter, we assume that each feature from the prior map partially can be changed. The proposed method considers the confidence of each feature extracted from the prior map by evaluating it with the current measurement. To evaluate the confidence of each feature map, the amount of information between the feature grid maps and sensor measurements is calculated according to entropy information theory [15]. For real-time operation, each amount of information is calculated from the weights of particles and is applied as gains of each feature in the particle filter.

To utilize vertical information from a 3D point cloud, the management of the 3D point cloud is important. Triebel *et al.* [3] proposed the MLS (Multi-Level Surface) map that includes multiple surface information in one cell of the grid map. In another work, Wolcott *et al.* [2] proposed multi-resolution Gaussian mixture maps that contain vertical information. Similar to the MLS map, this letter proposes an efficient management map of a point cloud to cover a large area by utilizing an image format.

This letter is organized as follows. The map representation and its management method will be described in Section II. Section III introduces our novel proposed fusion algorithm based on a particle filter using both road intensity and vertical information. Finally, we will present experimental results to demonstrate our proposed method and conclusions in Sections IV and V, respectively.

II. The Map Representation

In this section, a map representation method is introduced to generate a grid map that contains road intensity as well as vertical information. Additionally, an efficient map management strategy is also described to handle large scale areas such as a large city or even a whole country. Here in this letter, we will use the map data of one town area in Singapore provided by SLA, which will be introduced in Section IV.

Similar to the MLS algorithm [3], each cell of the grid map is constructed to contain vertical information from the ground by having upward grid cells. For localization, it is not necessary to save all vertical information. Therefore, cells of interest (COI) are selected by combining upward grid cells and a vertical gap from each ground grid cell as shown in Fig. 1. As vertical information near the ground is inaccurate, there is a vertical gap to ignore that vertical data. This approach can also save memory. In this letter, size of the ground cell, size of the upward cell, and the vertical gap are set as 10 cm, 50 cm, and 50 cm, respectively.

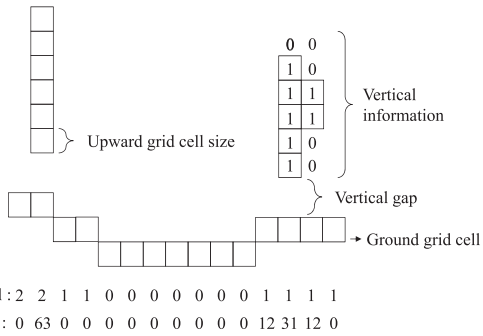

Fig. 1. The concept of the map representation method that includes the ground of road and vertical information from the road. In blue channel, the values are represented to elevation value, e.g., 2 means 2 × size of grid cell. In the red channel, the values represent occupancy of upward grid cells in binary bits, e.g., since the first right vertical occupancy is 001100 from the top, it can be represented as 00001100 in 8-bit binary system.

As multiple upward grid cells are associated with a ground grid cell, it is possible to extract a multi-layer vertical grid map.

The management strategy of the grid map is to utilize an image processing algorithm. The image processing technique is well developed for data compression, storage, and management. Thus, the essential information for localization is saved in basic image data comprising eight bits of RGB (red-green-blue) channels. The information, which should be saved in the grid map for localization, is intensity of the road, height of the road, and vertical information from the ground. The intensity and the height of the road are simply saved in a green and blue channels, respectively. To store these data, the road information first should be found from the prior point cloud by searching traversable surface patches. The traversable surface patches are determined by checking traversable neighboring cells, e.g., whether at least six cells have less than 10 cm height-distance among eight neighboring cells. For localization using vertical information, an occupancy grid map should be extracted from the upward grid cells at certain height. As one channel of an image has eight bits, the range of each element is limited to eight bits. The intensity value on the road is easily saved in a green channel by normalizing into eight bits. As the maximum value of eight bits is 255, the maximum capacity of the height of road is 255 × (the ground cell resolution), that is 25.5 m in this letter from the minimum height of the road. As the upward grid cells are required for full occupancy information, the eight upward COI are saved as binary bits. To help understand this concept, an example is illustrated in Fig. 1. The occupancy of binary bits in a red channel is filled with vertical information from the height of road according to the interesting upward grid cells. On the right side in the figure, there are two occupied upward grid cells (vertical information) on the two skipped upward grid cells. Data in the vertical gap are not counted at all. Thus, the binary value of the data is 00001100 in one byte representation that is 12 in decimal system. Similarly, the data of the second one from the right is 00011111 in binary and 31 in decimal system. In this letter, the capable range of vertical information is 0.5 m to 4.5 m from the ground which is sufficient to extract and store vertical grid map for localization.

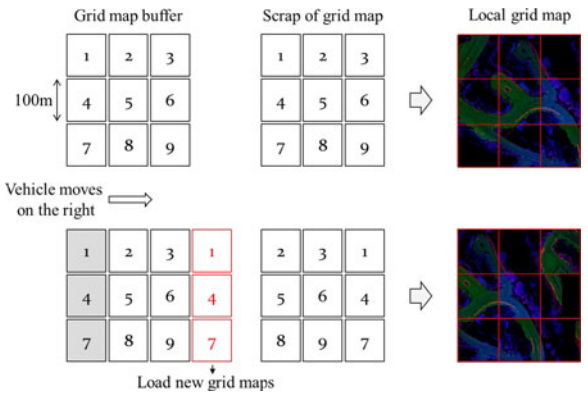

Fig. 2. The concept to load the grid maps dynamically. When the vehicle places at the middle of the grid map buffers as shown in the first column. The grid map patches around the vehicle are loaded. Then the local grid map is generated according to the scrap of grid maps. When the vehicle moves to the right grid buffer as shown in the second column, the new three grid maps patches are loaded and saved at the 1, 4, and 7 grid map buffers. Then, the new local grid map is generated according to the scrap of grid maps.

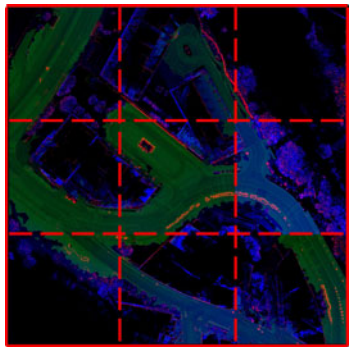

Fig. 3. The result of a grid map patch.

As the grid map is saved in a PNG (portable network graphics) image format, which involves lossless compression, the grid map is efficiently managed and stored. The image grid map patches (e.g., 1,000 $\times$ 1,000 pixels) are generated by cutting a certain size of the grid map. The image grid map patches can be easily managed and modified with any general image editing tool. Being saved in an image format, the road intensity and vertical features can be rapidly extracted from the image patches in real-time. Thus, it is possible to load the grid maps dynamically as shown in Fig. 2, during real-time running to save RAM memory. In Fig. 2, nine image grid map patches are loaded in grid map buffers around the vehicle pose. The local grid map consists of the nine pieces of patches from the grid map buffers. When the vehicle moves to the right side of the patch, three new grid map patches are loaded into the grid buffers such as 1, 4, and 7. The final local grid map result is shown in Fig. 3.

From the final grid map patch, a road intensity and multi-layer vertical grid maps are extracted as shown in Fig. 4. The road intensity grid map is extracted from the green channel of the patch and the multi-layer vertical grid maps are extracted from the blue and red channels. The road intensity grid map consists of high intensity data such as lines, arrows, and crosses.

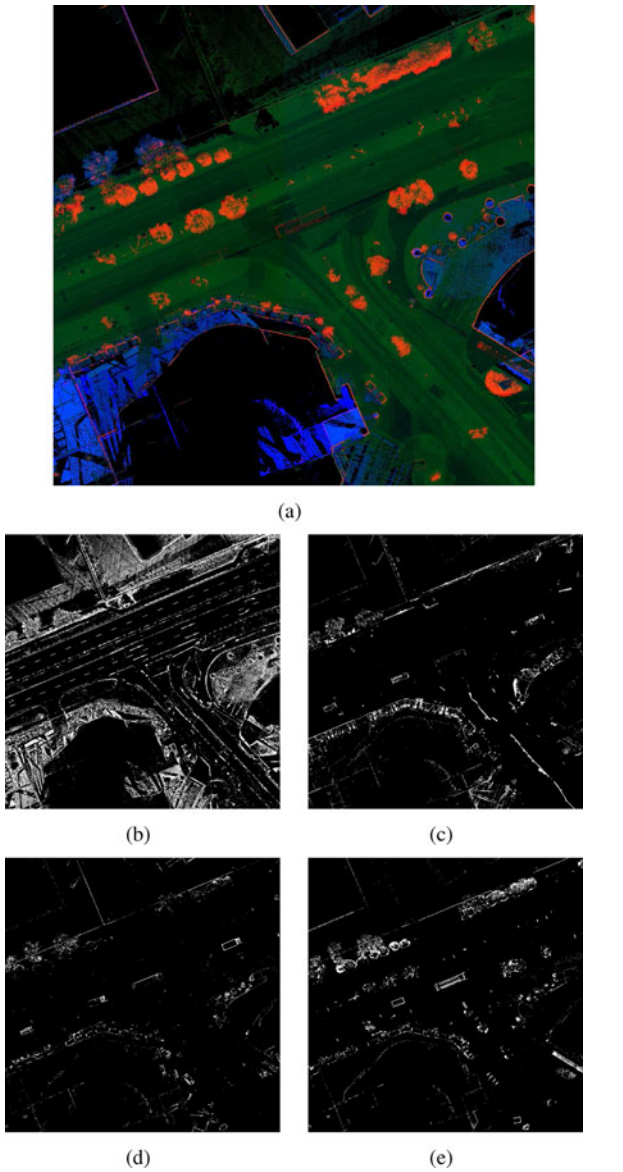

Fig. 4. (a) The original grid map image. (b) The road intensity feature map. (c) The first layer of vertical feature map ($0.5 <$ height ≤ 1.5). (d) The second layer of vertical feature map ($1.5 <$ height ≤ 2.5). (e) The third layer of vertical feature map ($2.5 <$ height ≤ 3.5).

The multiple layers can be generated by setting of upward grid cells. In this letter, three layers are generated depending on the height such as 0.5 m to 1.5 m, 1.5 m to 2.5 m, and 2.5 m to 3.5 m.

III. The Proposed Fusion Method

A. Localization With Particle Filter

This section describes an MCL algorithm [16] utilizing a road intensity and vertical grid maps from the image grid map. The features from sensor measurements for each grid map are extracted according to intensity data and height information.

In this letter, a particle filter or an MCL is utilized to optimize the weight functions of intensity and vertical information. The particles of MCL maintain three degrees-of-freedom (x, y, and

yaw), and the other elements (z, roll, and pitch) are estimated from an inertial measurement system and a normal vector of the ground plane in the grid map. The MCL algorithm is presented in Algorithm 1.

Firstly, the conventional MCL method is described. The k-th particle and its weight at time t are denoted as $x_t^{[k]}$ and $w_t^{[k]}$, respectively. All particles are initialized to the initial state x_0 according to the initial distribution while their weights are set to the same value. After initialization, the poses of particles are predicted by the $\mathbf{motion\_model}$ in line 6 using inertial sensors and odometry, u_t, according to the odometry motion model [16]. Since this letter utilizes a road intensity map as well as multi-layer vertical maps, there are several measurement updates: one for the road intensity map and the other for multi-layer vertical maps. The measurement, z_t, updates the k-th particle weight according to the $\mathbf{measurement}$ function as follows:

$$ {}^{(r,v)}w_t^{[k]} = \exp\left\{-\frac{1}{2}\cdot \mathrm{corr}\left(m^{(r,v)}, x_t^{[k]}, z_t^{(r,v)}\right)+1\right\} \quad (1) $$

where corr() function denotes the Pearson product-moment correlation coefficient, and the superscript r and v represent road intensity and vertical information, respectively. m and z denote a grid map and a measurement, respectively. In Algorithm 1, the subscript i in v denotes a multi-layer factor. After a normalization step for each weight, the final weight $w_t^{[k]}$ of all particles is updated by the sum of each weight in lines 14 and 18. According to [17], resampling is only performed when N_{eff} is less than a certain threshold η_{eff}, e.g., $0.8 \times N$, to avoid a degeneracy phenomenon.

Algorithm 1: The proposed MCL.

1: **Initialization:**
2: $x_0^{[k]} \leftarrow p(x_0), k = 1, \ldots, N$
3: $w_0^{[k]} \leftarrow 1/N, k = 1, \ldots, N$
4: **Iterations:**
5: **for** $k = 1$ to N **do**
6: $x_t^{[k]} = \mathbf{motion\_model}(u_t, x_{t-1}^{[k]})$
7: ${}^{(r,v)}w_t^{[k]} = \mathbf{measurement}(z_t^{(r,v)}, x_t^{[k]}, m^{(r,v)})$
8: **end for**
9: Normalization step s.t. $\sum_{k=1}^{N} {}^{(r,v)}w_t^{[k]} = 1$
10: $H(W_t^{(r,v)}) = -\sum_{k=1}^{N} {}^{(r,v)}w_t^{[t]} \log {}^{(r,v)}w_t^{*,[t]}$
11: **for** $k = 1$ to N **do**
12: **Conventional method:**
13: $\tilde{w}_t^{[k]} = {}^{r}w_t^{[k]} + \sum_{i=1}^{n} {}^{v_i}w_t^{[k]}$
14: **The proposed method:**
15: $\tilde{w}_t^{[k]} = (1 - H(W_t^{r})) \cdot {}^{r}w_t^{[k]}$
16: $+ \sum_{i=1}^{n} (1 - H(W_t^{v_i})) \cdot {}^{v_i}w_t^{[k]}$
17: $w_t^{[k]} \propto w_{t-1}^{[t]} \cdot \tilde{w}_t^{[k]}$
18: **end for**
19: Normalization step s.t. $\sum_{k=1}^{N} w_t^{[k]} = 1$
20: $N_{eff} = \left[\sum_{k=1}^{N} \left(w_t^{[k]}\right)^2\right]^{-1}$
21: **if** $N_{eff} \leq \eta_{eff}$ **then**
22: $\left[x_t^{[k]}, w_t^{[k]}\right] = \mathbf{Resampling}(x_t^{[k]}, w_t^{[k]})$
23: **end if**

B. The Proposed Entropy-Based Fusion Algorithm

This section describes a novel proposed fusion algorithm based on a particle filter. When estimating the weight of each particle in a conventional particle filter using multiple measurement models, weights from various measurement models are simply summed. However, the capability of each measurement model is totally different depending on the situation of the environment such as whether there being a change or lack of features. Therefore, this letter proposes a novel weighted sum method to estimate the weight of each particle from weights of different measurement models. In this respect, it is important to estimate the exploit of measurement models for optimization. In this letter, each measurement model calculates relevant information between the sensor measurement and a map based on entropy information theory.

Based on the entropy information theory, the entropy is calculated as follows:

$$ H(X) = -\int P(x)\log P(x)dx \quad (2) $$

where $P(x)$ is a probability mass function. As the cost function is non-linear, it is hard to calculate equation (2) in real-time. Thus, the entropy of each cost function is approximately estimated by the weights of particles as follows:

$$ H(W_t^{(r,v)}) = -\frac{1}{N}\sum_{k=1}^{N} {}^{(r,v)}w_t^{[k]} \log {}^{(r,v)}w_t^{[k]}. \quad (3) $$

The most different parts from the conventional method are lines 13, and 15–17 in Algorithm 1. After updating each weight of each particle, the entropy of each measurement model is calculated. The amount of information in the entropy of each measurement model is reversed because same values of weights means less information. Thus, the amount of information of each measurement is expressed as $1 - H(W_t^{(r,v)})$. Finally, the amount of information is updated as the weighted gains to generate the weight of each particle.

The reliability of each grid map is evaluated by the calculated information between the grid maps and feature measurements. As the reliabilities are applied as the gains for the weights of particles, a higher confidence grid map has greater contribution for localization. When some grid map includes significant change, the reliability of the grid map becomes low. For example, if road lines and arrows are redrawn due to road work, the amount of mutual information will decline because of the difference. The contribution of the intensity grid map will be small because the gain of its weight is reduced. Therefore, the proposed method can provide robust localization.

(a)

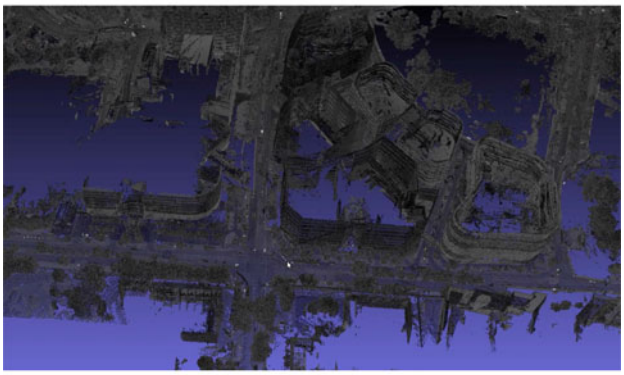

(b)

Fig. 5. (a) The whole point cloud data provided by SLA was overlaid on the Google map. (b) The close-range point cloud data around One-north in Singapore.

IV. Experimental Results

The high accuracy point cloud is provided by SLA(Singapore Land Authority) for 3.45 km^2 near One-north area in Singapore, as shown in Fig. 5(a). As shown in Fig. 5(b), the provided point cloud is extremely accurate. However, the data may have changed vertical as well as road intensity information because they were collected six months ago. The point cloud data consist of 6,292,573,705 points. The total size of data is 30.5 GB even though it is compressed in LAS/LAZ format, which is a public compressed 3-dimensional point cloud format. Through the generation process of a grid map, 380 image patches are generated. The total size of the image patches is 218.2 MB. The MLS algorithm [3], a reference algorithm for comparison, compresses 20,207,000 points to 57.96 MB. Therefore, the proposed algorithm has approximately 84 times better compression ratio than the conventional algorithm.

There are many constructions around the One-north area. The precise point cloud is collected in Nov. 2015 and the proposed algorithm was tested in May 2016. Since the prior map is outdated, especially in construction areas, there are many changed environments not only for the vertical grid map but also the road intensity grid map as shown in Fig. 8.

The proposed method was demonstrated through real environment data collected from the survey vehicle shown in Fig. 6.

Fig. 6. The survey vehicle equipped with Velodyne, GPS, IMU, and wheel odometry.

(a)

(b)

(c)

Fig. 7. (a) The five laps of 2.8 km loop around One-north area in Singapore. (b) A single loop of 4 km distance. (c) A single loop of 1.9 km distance.

The survey vehicle is equipped with Velodyne LiDAR (32E), IMU (KVH-1775), odometry, and high performance GPS (Applanix POS LV). The IMU and wheel odometry sensor are exploited to predict the vehicle pose and Velodyne LiDAR 32E is utilized as a measurement sensor. Although the high performance GPS has 2 cm and 1 degree accuracy in RTK (Real-Time Kinematic) mode, the RTK mode is rarely available in the test areas because of many skyscrapers. Therefore, the ground truth is generated by utilizing a graph optimization method with the high performance GPS, wheel odometry, and ICP (Iterative Closest Point) between measurements and the map off-line. The proposed method tested 19.9 km distance around One-north in Singapore as shown in Fig. 7.

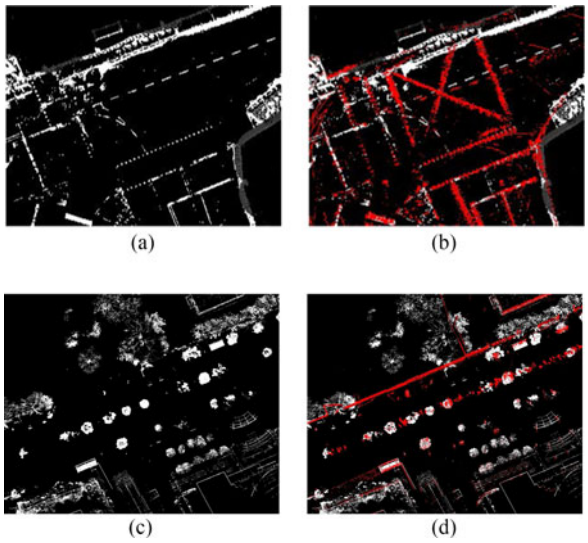

Fig. 8. (a) The outdated road intensity grid map from the prior map. (b) The current road intensity features (red) are overlaid on the outdated road intensity grid map. (c) The outdated vertical grid map from the prior map. (d) The current vertical features (red) are overlaid on the outdated vertical grid map.

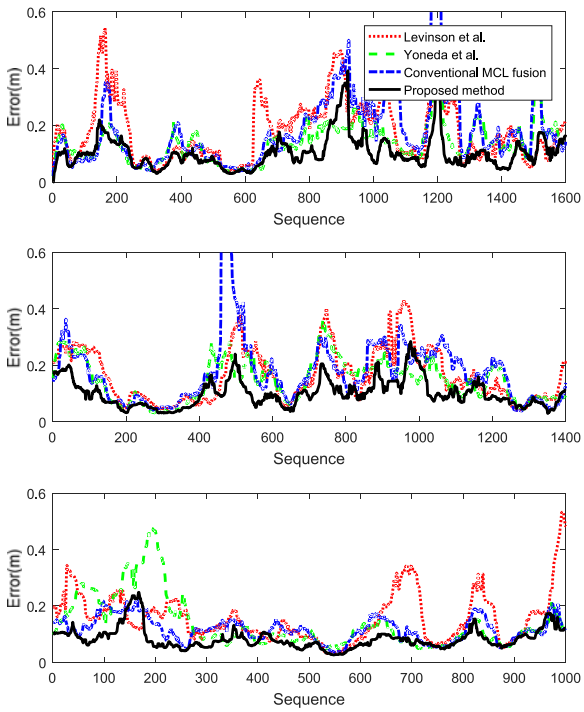

Fig. 9. The distance errors for the proposed and conventional methods for the three test sets.

To verify the superior performance of the proposed method, it is compared with several reference algorithms. As most autonomous vehicles utilize only road intensity data for localization, a classical general road intensity data-based MCL algorithm is chosen to be one reference algorithm [1]. As a state-of-the-art method, the algorithm of Yoneda *et al.* [12] is compared. Fig. 9 shows the geometric distance error of the proposed approach and the other conventional methods compared

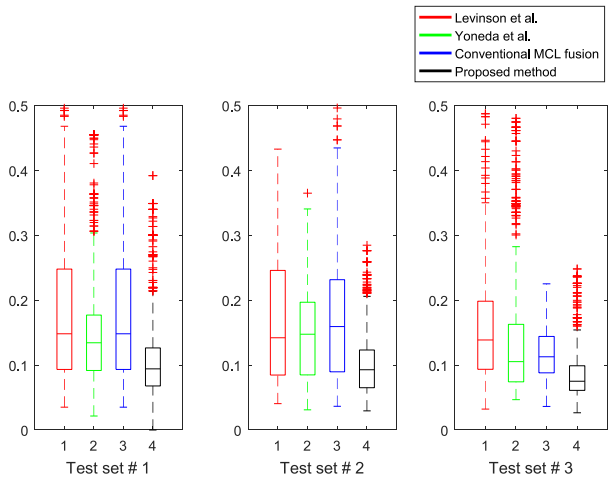

Fig. 10. The distance errors for the proposed and conventional methods for the three test sets.

TABLE I
COMPARISON OF THE PROPOSED METHOD AND THE OTHER CONVENTIONAL METHODS FOR EACH TEST SET (UNIT: METER, DEGREE)

	1st test set		2nd test set		3rd test set	
	Mean	Stdev	Mean	Stdev	Mean	Stdev
Levinson *et al.*						
x	0.125	0.125	0.128	0.130	0.085	0.091
y	0.129	0.135	0.113	0.107	0.128	0.124
θ	1.195	8.950	1.090	0.391	1.934	15.945
Yoneda *et al.*						
x	0.099	0.095	0.108	0.101	0.071	0.085
y	0.104	0.109	0.108	0.112	0.113	0.119
θ	1.442	8.927	1.199	0.396	2.045	15.939
Conventional fusion MCL						
x	0.121	0.117	0.142	0.165	0.062	0.068
y	0.128	0.156	0.120	0.120	0.104	0.092
θ	1.276	8.930	0.976	0.400	1.911	15.939
Proposed method						
x	0.075	0.071	0.077	0.073	0.047	0.054
y	0.082	0.098	0.070	0.068	0.071	0.066
θ	1.317	8.929	1.098	0.407	1.959	15.939

with the ground truth for each test set and Fig. 10 shows its box plot. The mean and standard derivation of each error are shown in Table I.

According to the amount of mutual information between the measurements and each grid map, the weighted gain is changed as shown in Fig. 11. From the figure, the contribution of the intensity feature is generally higher than the others. On the other hand, the 3rd vertical feature is less contributive than the others. From Figs. 9, 10 and Table I, the superior performance of the proposed method is verified by comparing with the other conventional methods in 19.9 km distance of test data sets. Therefore, the robustness of the proposed method is verified compared with the other conventional methods. Paired t-Tests were performed for each test set, and the p-values are shown in

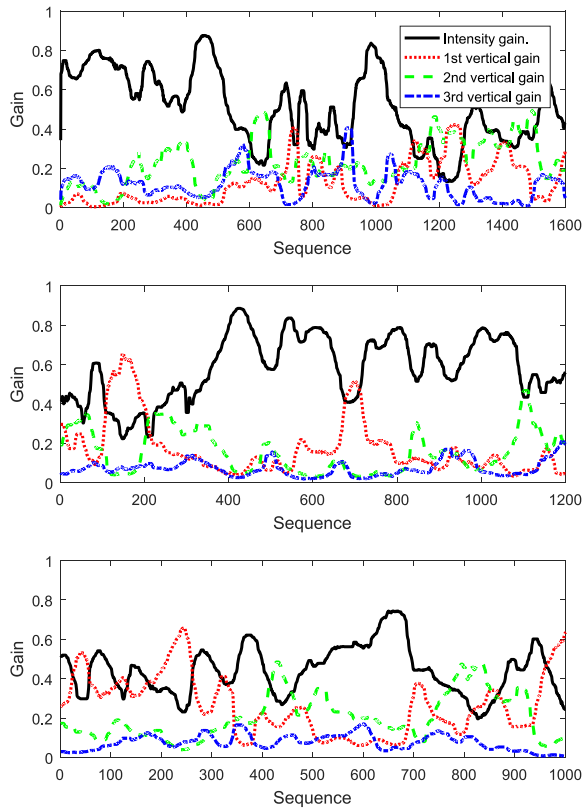

Fig. 11. The plot of gains for the weight sum through the three test sets.

TABLE II
THE p-VALUES OF PAIRED t-TESTS WITH EACH CONVENTIONAL METHOD

	Levinson *et al.*	Yoneda *et al.*	Conventional MCL fusion
1st set	1.161×10^{-124}	1.294×10^{-52}	6.811×10^{-92}
2nd set	1.904×10^{-106}	1.299×10^{-79}	2.319×10^{-92}
3rd set	1.563×10^{-116}	8.396×10^{-61}	1.329×10^{-69}

Table II for each test set. So the superiority of the proposed algorithm is statistically assured since the p-values are extremely small.

V. CONCLUSIONS AND FURTHER WORKS

this letter proposed a novel fusion algorithm based on a particle filter using entropy information theory. Since each measurement model is involved in the information gain, it can contribute to a better performance. this letter proposed how to measure the amount of information of each measurement model in real-time and how to incorporate it in a particle filter. Additionally, an efficient management strategy of a grid map including both vertical and road intensity information was proposed. To verify the robustness of the proposed algorithm, it is tested in various environments. The video clip for the proposed method is uploaded in YouTube website (link: https://youtu.be/Ioinn1AsLH0). The proposed method successfully tested the self-driving two times in the 3rd test loop without any human control.

There is a limitation in accuracy in the current localization system, because of communication delay, inaccurate sensor calibration, etc. Especially, when the vehicle moves fast, the error increases. For the further works, we need to solve these problems for more precise localization. Moreover, we will apply multiple sensor system for accurate localization.

REFERENCES

[1] J. Levinson, M. Montemerlo, and S. Thrun, "Map-based precision vehicle localization in urban environments," in *Proc. Robot., Sci. Syst.*, vol. 4, pp. 1–8, 2007.
[2] R. Wolcott and R. M. Eustice, "Fast LIDAR localization using multiresolution Gaussian mixture maps," in *Proc. IEEE Int. Conf. Robot. Autom.*, 2015, pp. 2814–2821.
[3] R. Triebel, P. Pfaff, and W. Burgard, "Multi-level surface maps for outdoor terrain mapping and loop closing," in *Proc. Int. Conf. Intell. Robots Syst.*, 2006, pp. 2276–2282.
[4] Mitsubishi Electric Corporation, "Mobile Mapping System–Highaccuracy GPS Mobile Measuring Equipment," 2013. [Online]. Available: http://www.mitsubishielectric.com/bu/mms/
[5] Aisan Technology Co. Ltd., "MMS by AISAN TECHNOLOGY," 2013. [Online]. Available: http://www.whatmms.com/
[6] M. Montemerlo *et al.*, "Junior: The Stanford entry in the urban challenge," *J. Field Robot.*, vol. 25, no. 9, pp. 569–597, 2008.
[7] C. Urmson *et al.*, "Autonomous driving in urban Environments: Boss and the urban challenge," *J. Field Robot.*, vol. 25, no. 8, pp. 425–466, 2008.
[8] J. Levinson *et al.*, "Towards fully autonomous driving: Systems and algorithms," in *Proc. IEEE Int. Conf. Intell. Veh. Symp. (IV)*, 2011, pp. 163–168.
[9] J. Levinson and S. Thrun, "Robust vehicle localization in urban environments using probabilistic maps," in *Proc. IEEE Int. Conf. Robot. Autom.*, May 2010, pp. 4372–4378.
[10] A. Schlichting and C. Brenner, "Localization using automotive laser scanners and local pattern matching," in *Proc. IEEE Int. Conf. Intell. Veh. Symp. (IV)*, 2014, pp. 414–419.
[11] K. Yoneda, H. Tehrani, T. Ogawa, N. Hukuyama, and S. Mita, "Lidar scan feature for localization with highly precise 3-D map," in *Proc. IEEE Int. Conf. Intell. Veh. Symp. (IV)*, 2014, pp. 1345–1350.
[12] K. Yoneda, C. Yang, S. Mita, T. Okuya, and K. Muto, "Urban road localization by using multiple layer map matching and line segment matching," in *Proc. IEEE Int. Conf. Intell. Veh. Symp. (IV)*, Jun. 2015, pp. 525–530.
[13] H. Deusch, J. Wiest, S. Reuter, D. Nuss, M. Fritzsche, and K. Dietmayer, "Multi-Sensor self-localization based on maximally stable extremal regions," in *Proc. IEEE Int. Conf. Intell. Veh. Symp. (IV)*, 2014, pp. 555–560.
[14] F. Caron, M. Davy, E. Duflos, and P. Vanheeghe, "Particle filtering for multisensor data fusion with switching observation models: Application to land vehicle positioning," *IEEE Trans. Signal Process.*, vol. 55, no. 6, pp. 2703–2719, Jun. 2007.
[15] E. T. Jaynes, "Information theory and statistical mechanics," *Phys. Rev.*, vol. 106, no. 4, pp. 620–630, 1957.
[16] S. Thrun, W. Burgard, and D. Fox, *Probabilistic Robotics*, Cambridge, MA, USA: MIT press, 2005.
[17] A. Doucet, S. Godsill, and C. Andrieu, "On sequential Monte Carlo sampling methods for Bayesian filtering," *Statist. Comput.*, vol. 10, no. 3, pp. 197–208, 2000.